1987

NASA/ASEE SUMMER FACULTY RESEARCH FELLOWSHIP PROGRAM

GEORGE C. MARSHALL SPACE FLIGHT CENTER
THE UNIVERSITY OF ALABAMA IN HUNTSVILLE

RAMAN SPECTROSCOPIC INVESTIGATIONS OF Hg-Cd-Te MELTS

Prepared by:	Anny Morrobel-Sosa
Academic Rank:	Assistant Professor
University and Department:	The University of Alabama Department of Chemistry
NASA/MSFC Laboratory: Division: Branch:	 Space Science Laboratory Low-Gravity Science Crystal Growth
NASA Colleagues:	Frank R. Szofran Sandor L. Lehoczky
Date:	August 24, 1987
Contract No.:	The University of Alabama in Huntsville NGT-01-008-021

ABSTRACT

Raman scattering measurements are reported for a series of $Hg_{1-x}Cd_xTe$ (with $x \lesssim 0.2$) materials from 295K (room temperature) to 1126K (up to and above their liquidus temperatures), and for $Hg_{1-x}Cd_xTe$ ($x = 0.3$) at 295K. The samples were contained in high-temperature optically-flat fused silica cell. Variable temperature measurements were effected in a three-zone, high-temperature furnace equipped with optical windows, and monitored externally by three independently programmable temperature controllers. All studies were made in the backscattering geometry using the 5145 A line of an Ar^+ ion laser, with incident power less than 250 mW, as excitation source. An intensity enhancement is observed for a mode in each of the compositions studied. The frequency of this mode varies with composition, 142 cm^{-1} for HgTe, and 128 cm^{-1} for both the $Hg_{1-x}Cd_xTe$ ($x = 0.053$ and 0.204) samples. In addition, a shift to lower frequency as a function of temperature is observed in all samples. This shift is most prominent for the $x = 0.053$ sample. The temperature dependence of these modes as the liquidus temperatures are achieved and surpassed for these samples is presented as being associated with a structural transition in the Hg-rich compositions of the $Hg_{1-x}Cd_xTe$ series. To our knowledge this is the first reported study of Raman scattering by phonons in the melts of these materials.

ACKNOWLEDGEMENTS

The author wishes to thank the NASA/ASEE Summer Faculty Fellowship Program, its Directors, Dr. Gerald R. Karr of UAH and Ms. Ernestine Cothran of NASA/MSFC, and staff for their enthusiastic support of the Program and its objectives.

Utmost gratitude is due to both of my NASA colleagues, Dr. Frank R. Szofran and Dr. Sandor L. Lehoczky of the Space Science Laboratory/Low-Gravity Science Division/Crystal Growth Branch for their sponsorship and support of this project; their help and guidance was invaluable. Particular thanks are also due to Mr. Ronald P. Harris for his assistance in providing quick solutions to unexpected problems. The efforts and kindness of all members of the Crystal Growth Branch are also acknowledged.

The support of Prof. Drury S. Caine, Chairman of the Department of Chemistry at The University of Alabama, is greately acknowledged for allowing me to pursue the opportunity provided in the participation of this program.

INTRODUCTION

The $Hg_{1-x}Cd_xTe$ alloy system has received considerable attention in recent years, as can be attested to by several reviews[1-3] on the subject, for their use as infrared detector devices.[4] The energy gap in these materials increases continuously (almost linearly) with cadmium composition, ranging from -0.3 eV (for x = 0, HgTe) to +1.6 eV (for x = 1, CdTe) and zero-gap crossover at 4.2K for x = 0.15. The corresponding spectral range can thus be tuned with alloy composition from 0.8 m to 50 m. In particular, the x = 0.20 alloy has an atmospheric window of 8 m to 14 m at 77K. These materials have therefore been mostly considered for military, space and commercial applications. It is then not surprising to note that a significant proportion of past and present research efforts has been dedicated to the advancement of photodetector technologies and of crystal growth techniques.[2,5-7] These studies have, in turn, generated enormous interest in the characterization of basic physical proerties for this pseudo-binary alloy system.

Recent reports of variations in the thermal conductivities between the solid and melt,[6-8] changes in the melt thermal conductivity as a function of temperature and composition,[9,10] and increases in the thermal diffusivity with temperature,[10,11] are of particular interest to the work presented here, for they suggest possible chemical or structural changes in the melt structure near and/or above the liquidus temperatures. Optical studies of these materials are of clear significance since they reflect the nature of their electronic and vibrational structure. These efforts have concentrated on three spectroscopic techniques: infrared,[12-21] Raman,[21-26] and resonance Raman[27-29] scattering. The temperatures at which these studies were made range between 1.7K to 300K, the maximum temperature. All of the Raman studies have included the materials with $0 < x < 0.3$ composition; yet, none of the resonance Raman scattering investigations fall within this range. These reports have revealed a "two-mode"[30] behavior in the alloys arising from HgTe-like and CdTe-like modes which exhibit composition-dependent frequency shifts. Clustering and defect modes have also been detected[23-26] suggesting that surface morphology, such as structural dislocations, composition gradients, and surface preparation, can be studied by these techniques.

In this report we present what to our knowledge is the first study of Raman scattering by phonons in $Hg_{1-x}Cd_xTe$ melts. We have performed these studies on alloy

compositions of x = 0, 0.05, and 0.20, from room temperature, 22 °C (295K), up to and above their liquidus temperatures, 670 °C (943K), 703 °C (976K),and 794 °C (1067K), respectively. We also report the room temperature spectrum for x = 0.30 as the first step in a similar investigation to be performed on this alloy composition. The most salient feature in our study is the observation of an intensity enhancement of a phonon mode in each sample composition near and above its liquidus temperatures. We believe this mode to be indicative of a structural phase transition as suggested by others.[6-11] The mechanism for this transition has not yet been identified, though these results, preliminary as they are, do not indicate a soft phonon mechanism as being responsible for the structral transition.

OBJECTIVES

The primary purpose of this effort is the characterization of the liquid structure of $Hg_{1-x}Cd_xTe$ ($x \leq 0.30$) near and above the liquidus temperatures of each alloy compsition by means of Raman scattering spectroscopy. The project was motivated by previous observation[6-11] as discussed earlier. The technique of Raman scattering was chosen to perform this study for it probes lattice vibrations, phonons, and is very sensitive to the local structural environment. In what follows is a brief theoretical introduction and description of the technique and its relevant parameters. It is suggested that other authors be consulted for a detailed treatement of the phenomenom,[34-36] and in particular, for the case of semiconductors.[27,37-41]

The Raman effect[42] results from the inelastic scattering of light (of a given frequency, ω_o) by the molecular vibrations and lattice vibrations (in the case of dense media) of a medium. The scattered light consists of several frequency components, ω_j, and their corresponding frequency shifts, $\Delta\omega_j = \omega_o - \omega_j$, are characteristic of the material and independent of the choice of incident light frequency (except for the case of resonance light scattering). This frequency spread is identified by two regions, Stokes scattering ($\Delta\omega_j > 0$) and anti-Stokes scattering ($\Delta\omega_j < 0$). Since the populations are governed by the Bose-Einstein relationship, the intensities of the Stokes components are usually greater than those of the anti-Stokes components, they are the ones most frequently measured in Raman spectroscopy.

In the simplest case of an isolated, free, atom or molecule, the total intensity of scattered light for an optical transition from a state m to a state n is given by:

$$I_{mn} = \frac{2^7 \pi^5}{3^2 c^4} I_o (\nu_o \pm \nu_{mn})^4 \sum_{k,l} |(\alpha_{kl})_{mn}|^2$$

in the Kramers-Heisenberg-Weisskopf formalism. The incident radiation intensity and frequency are I_o and ν_o, respectively. $(\nu_o \pm \nu_{mn})$ is the scattered light frequency, where $\nu_{mn} = \nu_m - \nu_n$, and k and l are molecular fixed coordinates that characterize the scattered and incident light, respectively. $(\alpha_{kl})_{mn}$ is a complex, non-centrosymmetric polarizability tensor defined[43] as:

$$(\alpha_{kl})_{mn} = \frac{1}{h} \sum_r \frac{(\langle n|\hat{\mu}_k|r\rangle \langle r|\hat{\mu}_l|m\rangle + \langle n|\hat{\mu}_l|r\rangle \langle r|\hat{\mu}_k|m\rangle)}{(\nu_{rm} - \nu_o + i\Gamma_r)} \frac{}{(\nu_{rn} + \nu_o + i\Gamma_r)}$$

where: $\hat{\mu}_k$ and $\hat{\mu}_l$ are electric dipole moment operators in the k^{th} and l^{th} polarization, respectively, and Γ_r is the damping constant for the intermediate state(s), accounting for its finite width(s). The wavefunctions $|m\rangle$, $|n\rangle$, and $|r\rangle$ are eigenfunctions of the total Hamiltonian. The summation is performed over all the vibronic states of the molecules, including m and n, so as to consider the contributions from all electronic levels and their corresponding vibrational levels. In this treatment the wavefunctions are usually expanded in terms of the transition moments and generalized coordinates to obtain final expressions for the intensities of the Raman fundamentals and overtones.

Recently, extensions of the theoretical developments by Hayes and Loudon[34] have been presented for the specific case of Raman and resonance Raman scattering in semiconductors.[27,38-41] In this case, and for a similar experimental configuration as used in our study, the rate of scattered photons "inside" the sample per unit solid angle is given by:

$$\frac{d R_s^{in}}{d \Omega} = \frac{I_o}{\hbar \omega_o} \frac{d\sigma}{d\Omega}$$

where R_s^{in} is the scattered photon rate (photons/sec) inside the sample, Ω, is the unit solid angle and $d\sigma/d\Omega$ is the differential cross-section. The corresponding scattering rate "outside" the sample, which are experimentally measured as the area of the observed Raman peaks, can then be expressed in terms of the polarizability tensor[27,39,40] as:

$$R_s^{out} = \frac{T_o T_s P_o \omega_s^3}{(a_o + a_s) \eta_o \eta_s} \frac{\Delta\Omega^{out} N(\omega_{ph}) + 1}{2 c^4 \omega_{ph} M V_c} |\alpha_{os}|^2$$

where T_o and T_s are the incident and scattered transmission coefficients, a_o and a_s are the absorption coefficients at the incident and scattered frequencies, and η_o and η_s are the indices of refraction at the incident and scattered frequencies. (It is important to note that these parameters are temperature dependent). P_o is the incident laser power. ω_{ph} is the observed phonon frequency and $N(\omega_{ph})$ is the phonon occupation number. ω_s is the scattered photon frequency, $\Delta\Omega^{out}$ is the constant collection solid angle, and α_{os} is the Raman polarizability tensor. M and V_c are the reduced mass of the unit cell and the primitive cell volume, respectively.

While this analysis has been applied successfully for resonance Raman scattering in $Hg_{1-x}Cd_xTe$ ($x = 0.966$) at

100K,[27] only one study has been performed at high temperatures, for Si.[39] In this latter case, the data show a decrease in Raman signal intensities with increased temperature, while a resonance enhancement is observed with temperature dependent shifts and broadenings.

Ii is of interest to extend this theoretical treatement to the Raman scattering at high temperatures for $Hg_{1-x}Cd_xTe$ of $x \leq 0.3$ to aid in the elucidation of the melt structures. The experimental studies reported here are the initial efforts in such a study.

EXPERIMENTAL

The samples used for this study were provided by NASA from a series of previously prepared materials (see Table 1).[9] Each alloy was prepared from purified elements and loaded in-situ (inside a rocking-furnace to provide homogenization) into specially designed high-temperature, high-pressure, optically flat, fused silica cells (see Figure 1).[44] The last four sample cells listed in Table 1 (numbers 5, 6, 7, and 8) were selected for these measurements based on the quality of the cell surface. The cell configuration and the high reflectivity of the samples were among the factors considered in the determination of the optical configuration to be used.

Variable temperature measurements were performed with a three-zone, high-temperature furnace designed and built at NASA.[45] A cross-section of this furnace is shown in Figure 2.[46] The sample is attached to or placed in a sample holder and located in the middle zone. Optical access is effected through coated heat rejection windows.

Each zone is independently controlled and its temperature monitored by a programmable temperature controller (Barber-Colman model no. 570). These three controllers allow for the establishment of sequential programming (up to eight sequences within each of four possible programs) of a desired starting temperature, an end temperature (both in degrees Centigrade) and sequence duration (in fractions or multiples of minutes or hours). Any program-sequence can be initiated, held constant or stopped at any given time.

The sample cells were handled with polyethylene gloves and thoroughly cleansed with ethanol (99.9%) prior to placing inside the furnace cavity. This is required to avoid cell cracking or damage due to dust or excess sodium. Since the alloys expand upon freezing, every effort was made to maintain a temperature gradient throughout the zones. For all temperatures, other than at or very near room temperature, the top zone was maintained at temperatures hotter than the middle zone and it, in turn, kept hotter than the bottom zone. All samples were heated at a rate of approximately 1 ^{o}C/min., allowing for the temperature differences. Each zone was also allowed to achieve equilibrium by holding the temperatures constant at several intervals. It was during these intervals, which lasted between thirty and ninety minutes, that the spectra were recorded. After the alloys were completely liquefied, the samples were rapidly quenched (by cutting-off all electrical

Figure 1:
SAMPLE CELLS

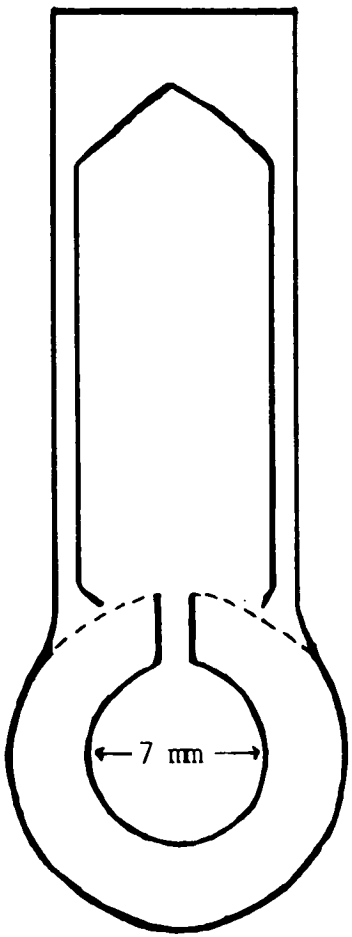

FRONTAL VIEW

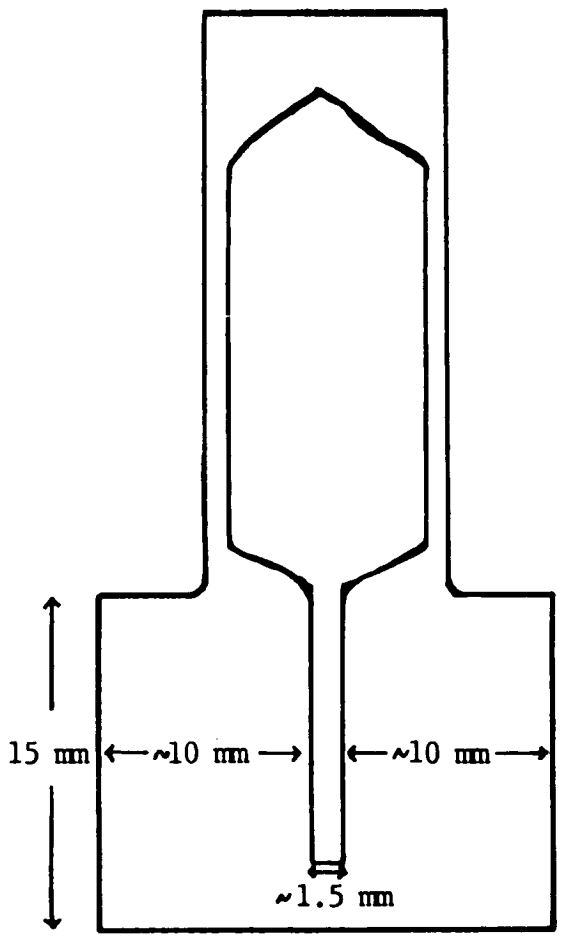

SIDE VIEW

Table 1

#	X	Solidus (°C)	Liquidus (°C)	Thickness (mm)
1	0.205	707	794	1.371
2	0	670	670	1.797
3	0.051	679	702	1.341
4	0.107	689	731	1.412
5	0.301	727	841	1.485
6	0.204	707	794	1.438
7	0	670	670	1.161
8	0.053	679	703	1.221

Figure 2:

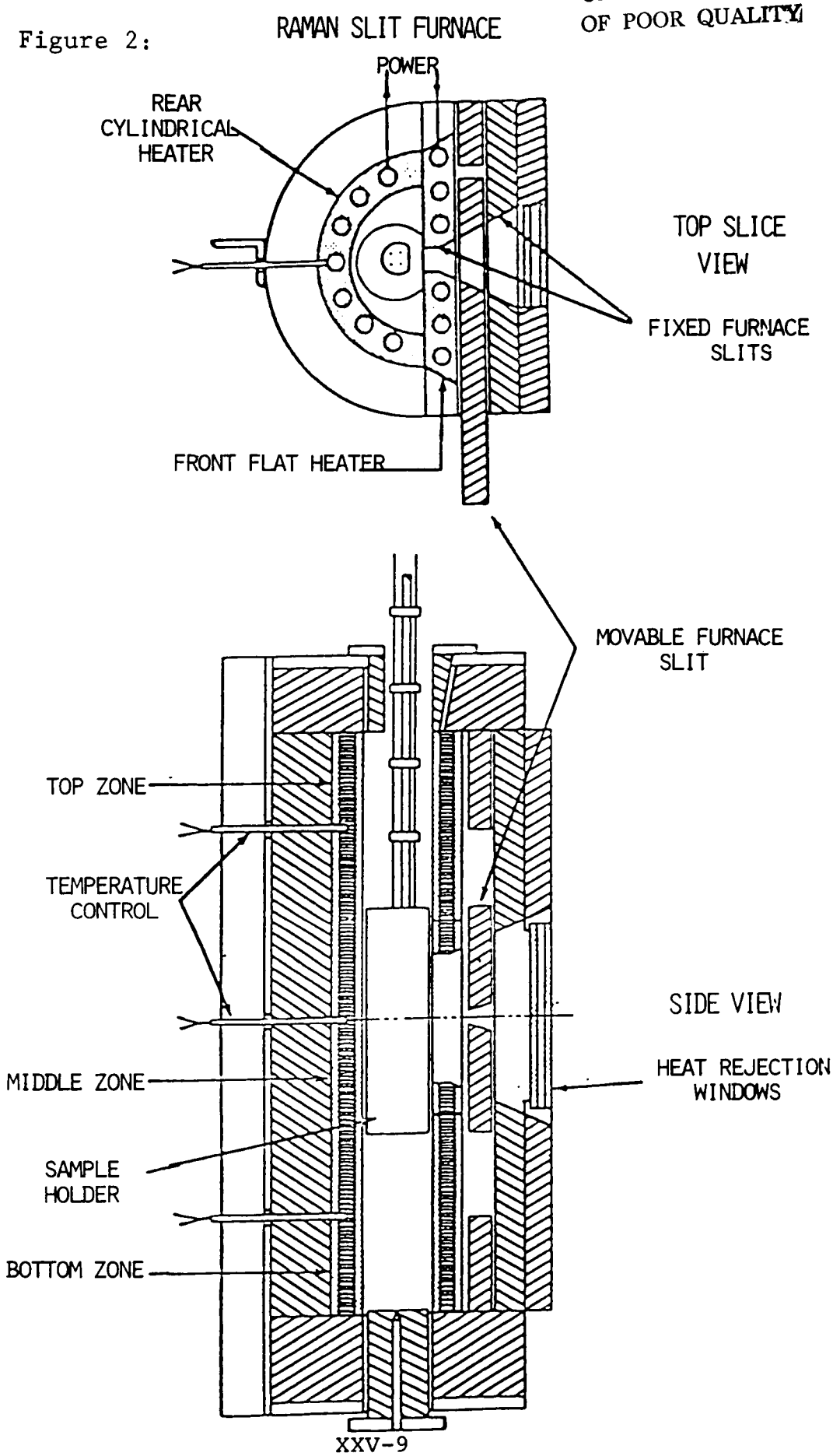

power to the furnace) to avoid CdTe segregation in samples where $x > 0$.

The cells were fixed in place by the sample holder. Two different sample holders were used during the course of this work (see Figures 3,[46] and 4), each with at least three type-K (chromel-alumel) thermocouples used to monitor either the three zone temperatures, or the top, middle and bottom of the cells, respectively. The thermocouple outputs were connected to a data acquisition/control unit (Hewlett-Packard model no. 3497A) via a 20-channel thermocouple acquisition plug-in assembly (Hewlett-Packard model no. 44422A). The HP-3497A was interfaced to a personal computer (Hewlett-Packard model no. 85B). A computer program, originally developed by F. R. Szofran and modified for these purposes, was used to evaluate voltage-to-temperature conversions with respect to an internal reference, and plot temperatures, from various channels, versus selected acquisition time intervals. Temperature stability was maintained to an uncertainty of $\pm$ 2 ^{o}C.

The experimental configuration used for the measurements reported here is shown in Figure 5. The 5145 A line of a continuous-wave argon ion laser (Spectra Physics model no. 165) was used as the excitation source. The positioning optics consisted of a double-mirror combination to raise the laser beam to the same plane as the spectrometer slit, an iris and an optical filter that rejects all but the 5145 A line. The incident laser beam was then focused with a cylindrical lens (focal lenght of 300 mm), reflected by a small front-surface mirror into the furnace and onto the sample. This focuses the beam into a rectangular cross-section, or line image, parallel to the spectrometer entrance slit. The incident laser power was maintained at or below 250 mW to further diminish background scattering from entering the spectrometer. This is best achieved by operating the laser in the light (power-stabilized) mode.

The scattered light is then collected and focused by a double lens assembly (focal length of 300 mm), placed immediately behind the small mirror, and a single lens (focal length of 254 mm). This lens combination (see Figure 6) offered a good match with the spectrometer optics. The 0.85 m double monochromator (Spex model no. 14018) was equipped with 1800 grooves/mm gratings. The spectrometer slit settings are very important in determining the experimental resolution; but, another equally important factor is the total amount of signal collected and used for detection. Since the use of the backscattering geometry technique, in which both the incident and scattered light

Figure 3: ISOTHERMAL SAMPLE HOLDER

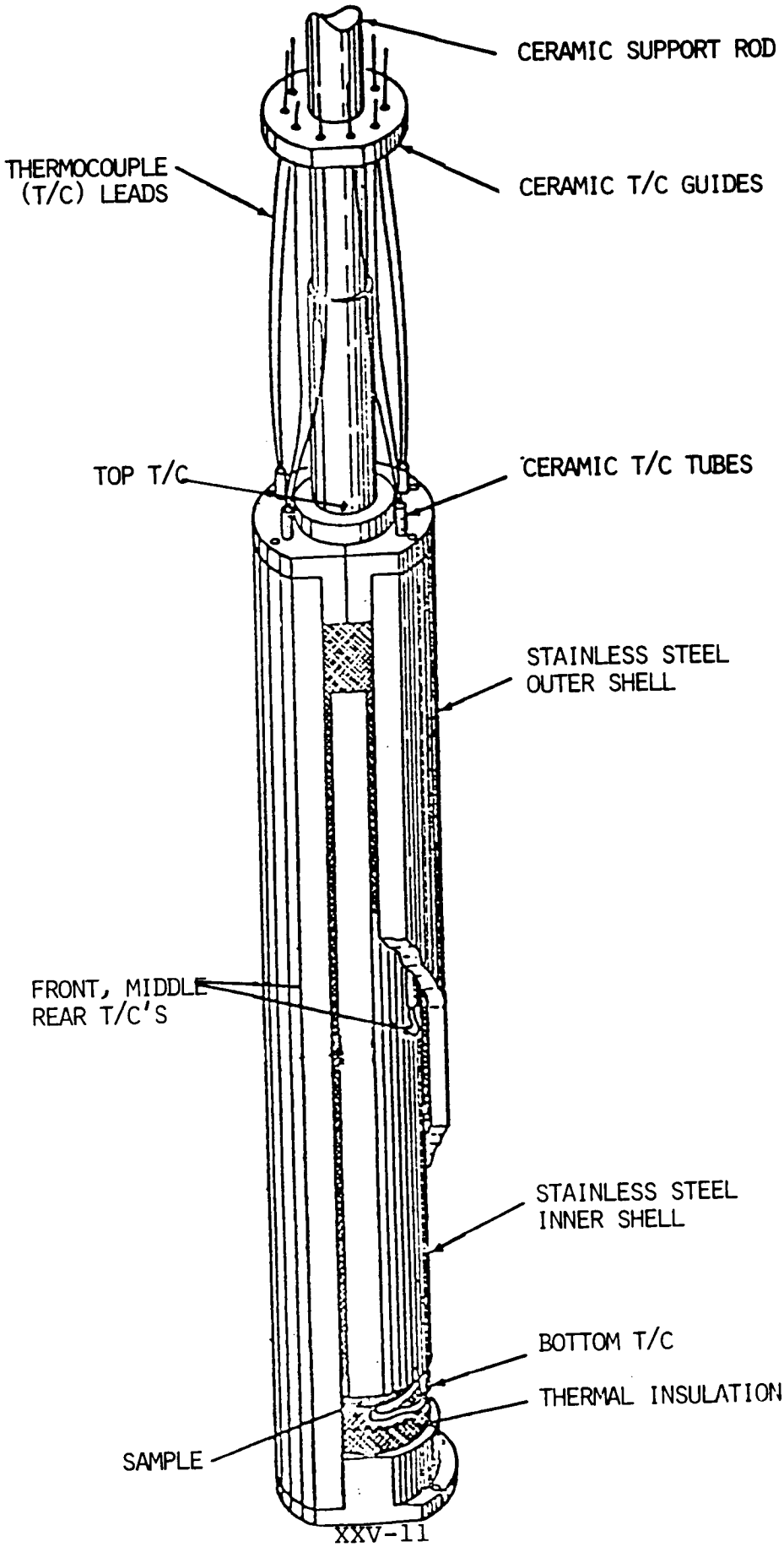

Figure 4: SAMPLE HOLDER

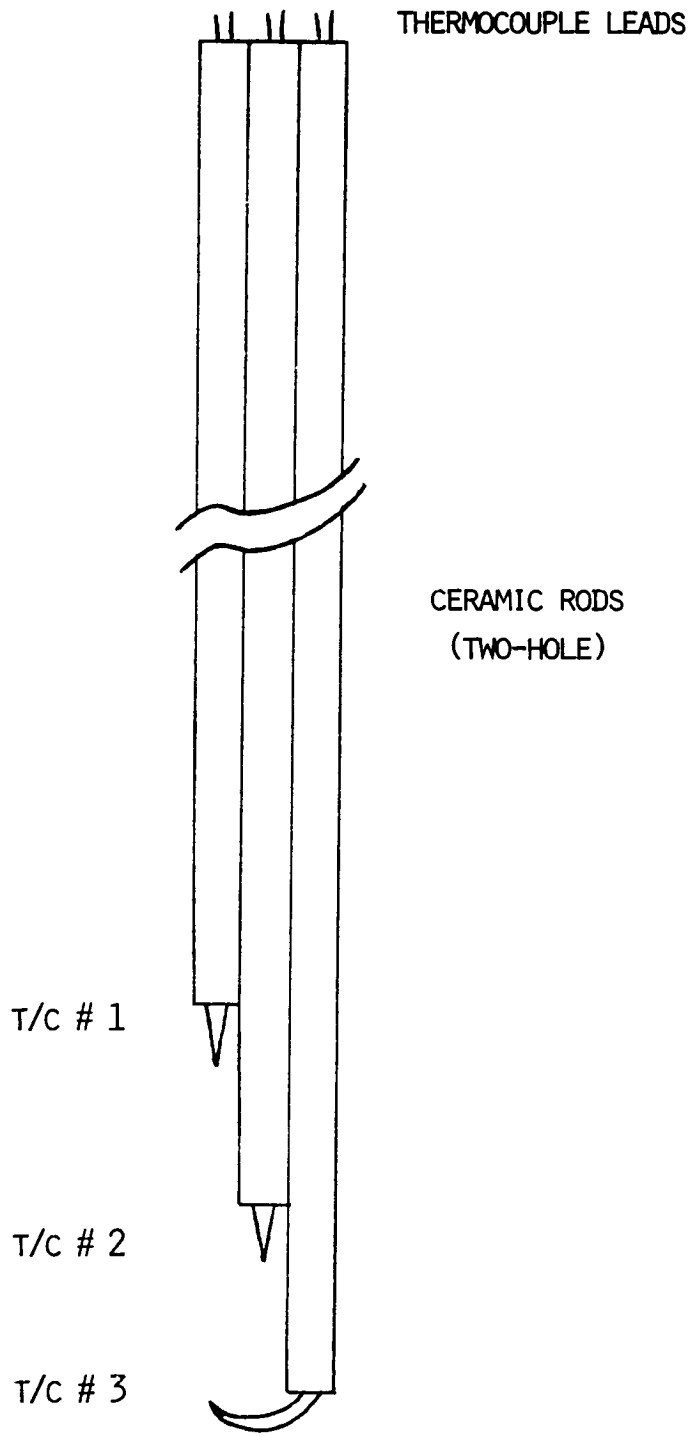

Figure 5: SCHEMATIC OF EXPERIMENTAL CONFIGURATION

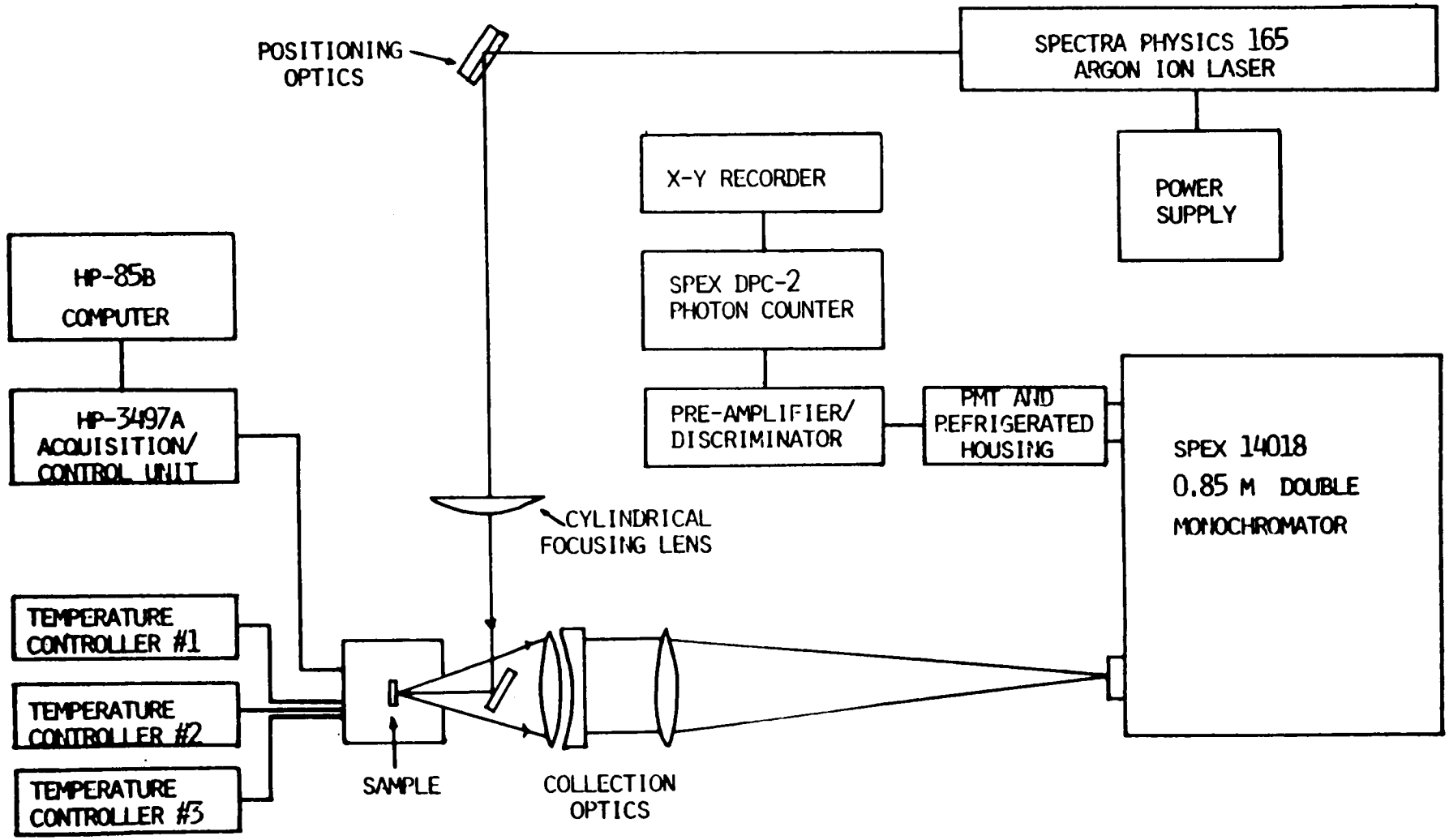

Figure 6: SCHEMATIC OF LASER PROBE AND BACKSCATTER COLLECTION OPTICS

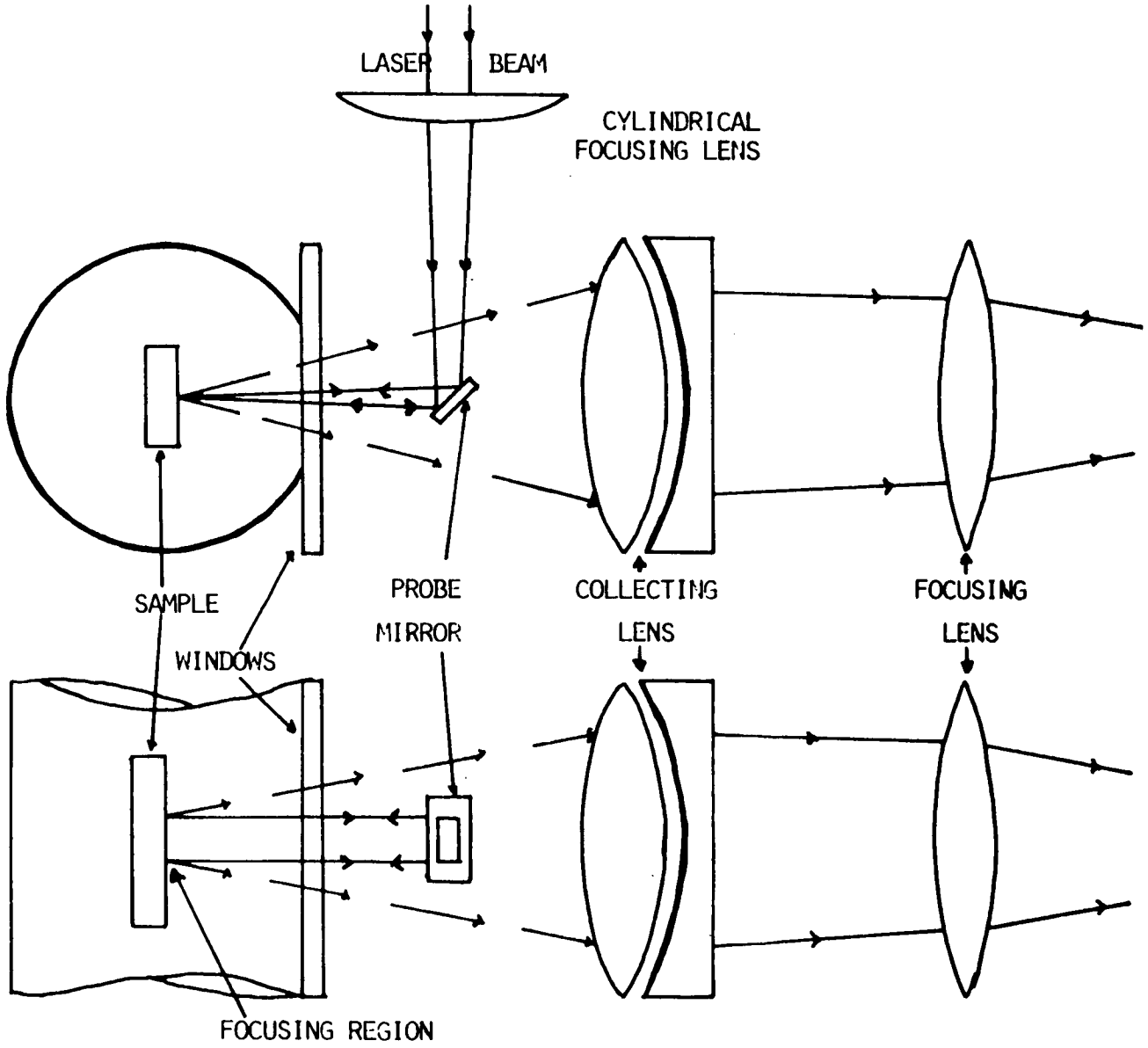

are co-linear, also allows for a line image focus onto the spectrometer slit. The entrance slit was kept at settings that would allow for a maximum collection of the scattered light. Typical settings were 0.5 mm - 1.0 mm - 0.5 mm slit widths for the three spectrometers slits and fully opened (2 cm) slit-height. Thus, a major portion of the scattered signal is collected at the sacrifice of increased spectral bandpass (approximately 5-6 cm^{-1}).

The advantages and disadvantages of the backscattering technique have been describe by others.[47-49] The primary concerns for this work are excitation/collection from only one, reflective sample surface, vertical line focus and minimization of local heating. It should be noted that caution is required to prevent direct laser beam reflection into the spectrometer and detector. This can cause unwanted laser-line ghosts, swamp the Raman signals in addition to possible damage to the detector.

The signals were detected by a refrigerated (-45 °C) photomultiplier tube (EMI tube model no. 9658 RAM, and housing model no. CH-25). The output is fed into a pre-amplifier/discriminator and into a digital photon counter (Spex model no. DPC-2). Typical dark counts were less than 200 counts/sec, while signals were on the order of 10^5 counts/sec. The spectra were then recorded by scanning the spectrometer (0.2 cm^{-1}/sec) and displayed on an X-Y recorder (Hewlett-Packard model no. 7034A or 7044A).

A series of preliminary procedures were undertaken prior to the performance of the experiments discussed here so as to ensure a successful outcome. The double monochromator was calibrated with a 200W Hg-Xe arc lamp (Oriel model no. 8500). Optical alignments of the experimental configuration was effected by removing the photomultiplier tube and replacing it wiht a low-power He-Ne laser (Spectra Physics model no. 155A). This back-alignment procedure was used to determine and optimize the optical path to be used for the optics and sample positions relative to the Ar^+ ion laser beam. To confirm that this optical arrangement was feasible for detection of Raman signals, carbon tetrachloride (CCl_4) was loaded into a sample cell similar to those used in these experiments and placed inside the furnace in a manner typical of the configuration to be used later. The expected Raman bands ($\sim$214, 314, and 460 cm^{-1}) were easily detected. Subsequently, preliminary runs with all the samples at room temperature were performed. Adequate safety precautions were also taken. A vented plexi-glass enclosure was designed around the upper part of the furnace, and near the working station. This

provides adequate operator safety in the event of a sample cell explosion.

RESULTS

The results are reported not in chronological order, but in order of increasing Cd composition for clarity. Preliminary measurements were performed on all samples to discern the most likely candidate for which strong Raman scattering signals could be obtained. Once this was established we proceeded in order of increasing liquidus temperatures. All temperature measurements were performed for one sample at a time.

A. HgTe

The Raman spectra of the HgTe sample for various temperatures are shown in Figures 7, 8, and 9. All spectra were recorded with increasing temperature and a spectral bandpass of 5 cm^{-1}. The most salient features are the decrease in intensity and shift towards lower frequency of the room temperature 128 cm^{-1} peak, the shift towards lower frequency of the very broad (18 cm^{-1}) band centered around 254 cm^{-1}, and the appearance of a strong broad (8 cm^{-1}) peak centered around 142 cm^{-1} with increasing temperature. The intensity enhancement of this latter band is most evident in the region between 700 ^{o}C and 751 ^{o}C. The difference between the two spectra recorded at 700 ^{o}C (see Figure 9) is that the uppermost spectrum was taken after a refocusing of the optics for the lower spectrum. This effect was also noticed for all other recorded Raman spectra as the liquidus temperatures were approached from below and surpassed. This may be due to an actual sample shift or settling in the molten state.

B. $Hg_{0.95}Cd_{0.05}Te$

The Raman spectra as a function of temperature for the 5% Cd composition sample are shown in Figures 10 through 14. As in the previous examples, all spectra were obtained with a spectral bandpass of 5 cm^{-1}. The 128 cm^{-1} peak observed in the HgTe sample is also detected here, but the shift towards lower frequency as well as the decrease in intensity with increasing temperature is most prominent in this sample. The shift is about 35 cm^{-1}. This is equally true for all features observed in the spectra. It should be noted that during the heating and detection sequence for this sample several adjustments in the optical focus had to be made. This may account for the different lineshapes observed for the same features, and for the almost dissappearance of any detectable signal between 597 ^{o}C and 704 ^{o}C.

Figure 7

HgTe

$\lambda_{exc.}$ = 5145 Å

1.0 M PC/s

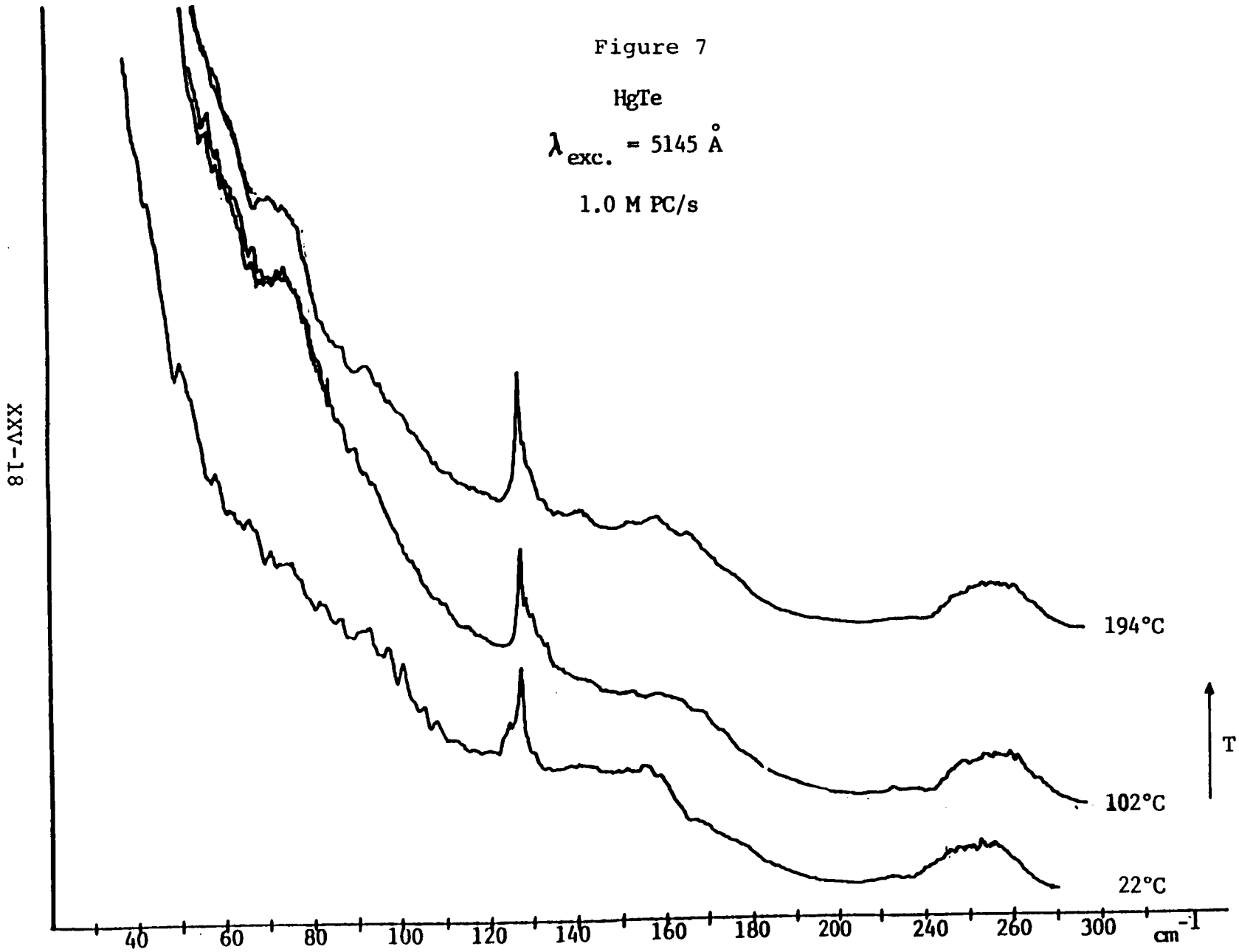

Figure 8

HgTe

$\lambda_{exc.}$ = 5145 Å

1.0 M PC/s

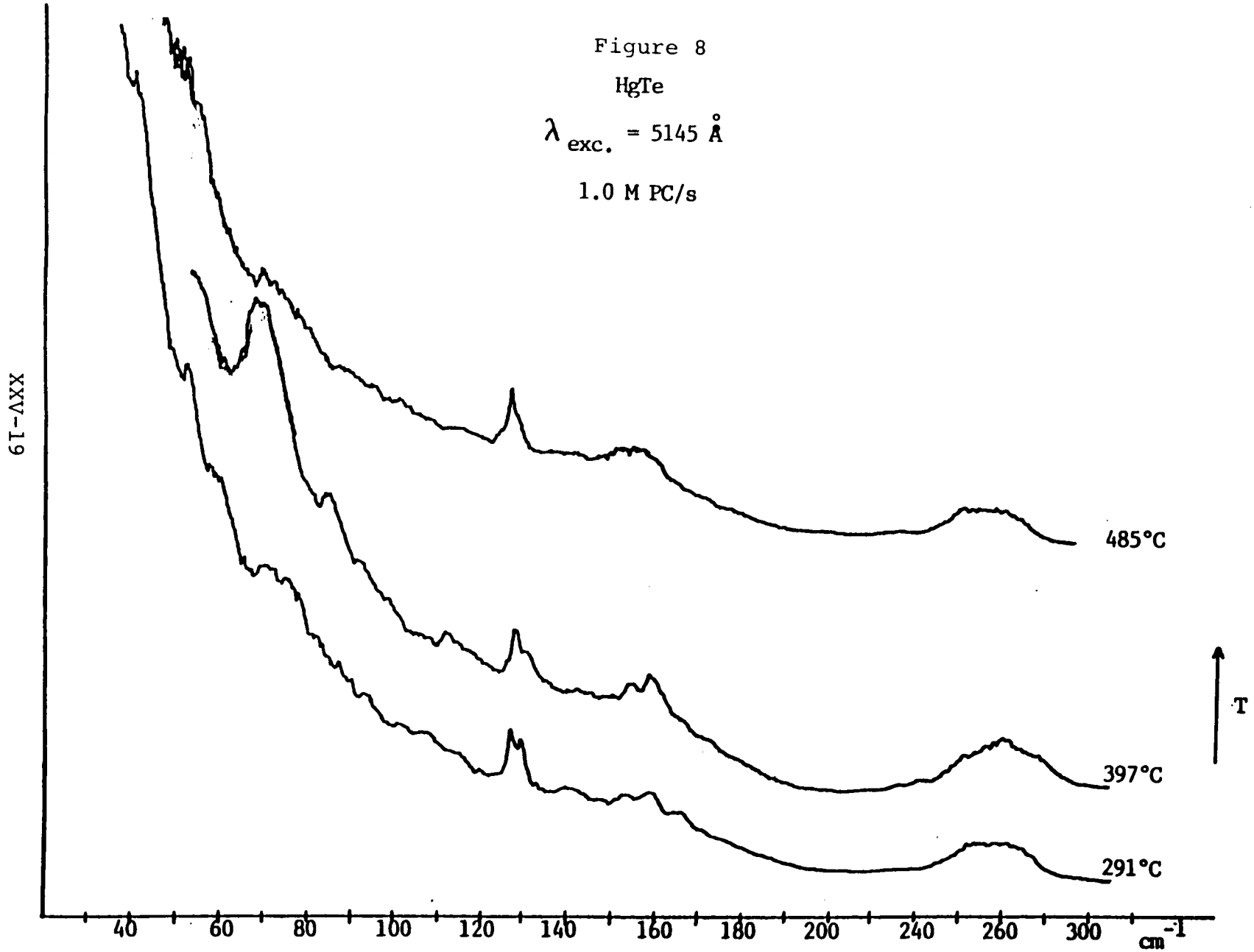

Figure 9

HgTe

$\lambda_{exc.}$ = 5145 Å

1.0 M PC/s

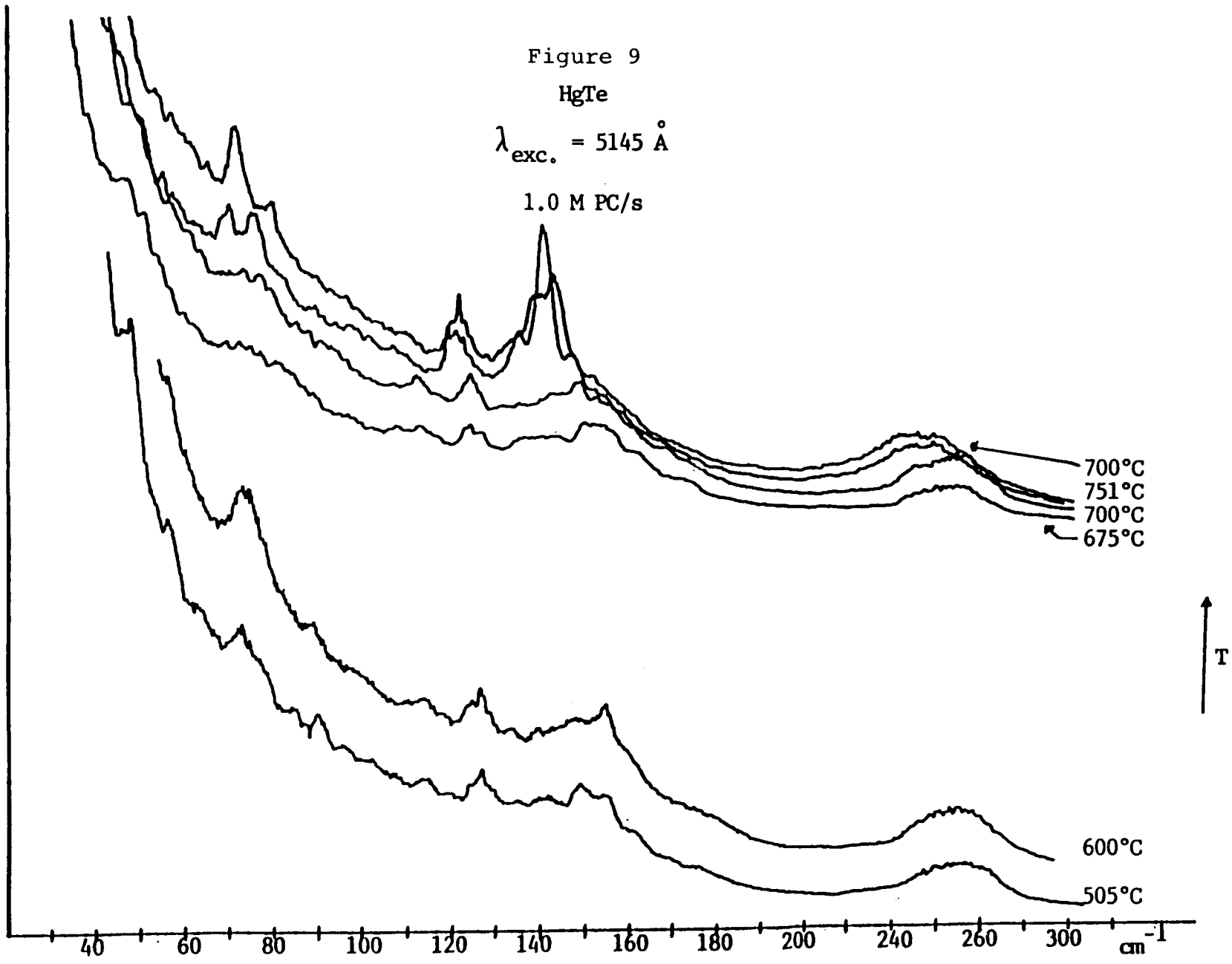

Figure 10

$Hg_{1-x}Cd_xTe$ (x = 0.053)

$\lambda_{exc.}$ = 5145 Å

0.5 M PC/s

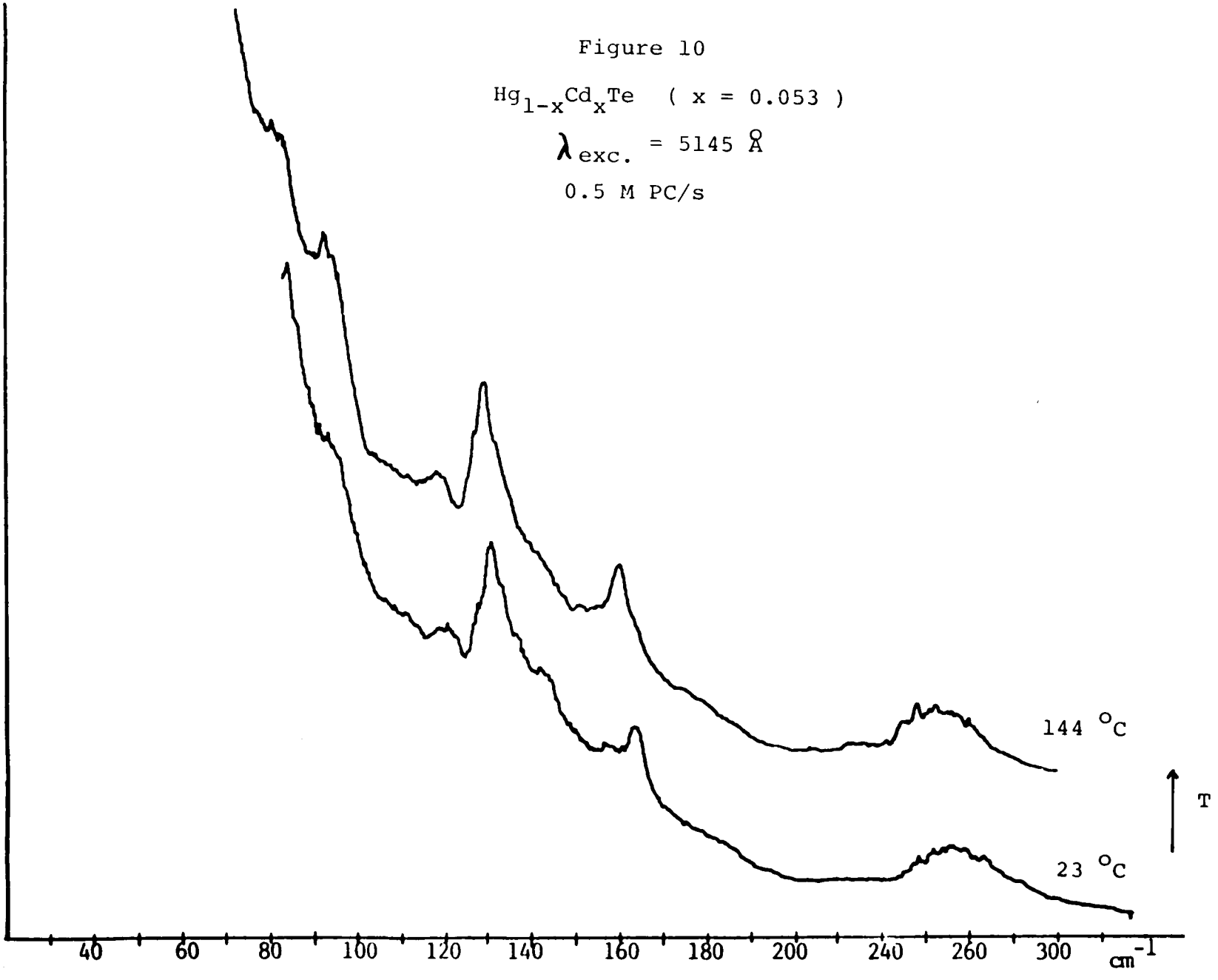

Figure 11

$Hg_{1-x}Cd_xTe$ (x = 0.053)

$\lambda_{exc.}$ = 5145 Å

1.0 M PC/s

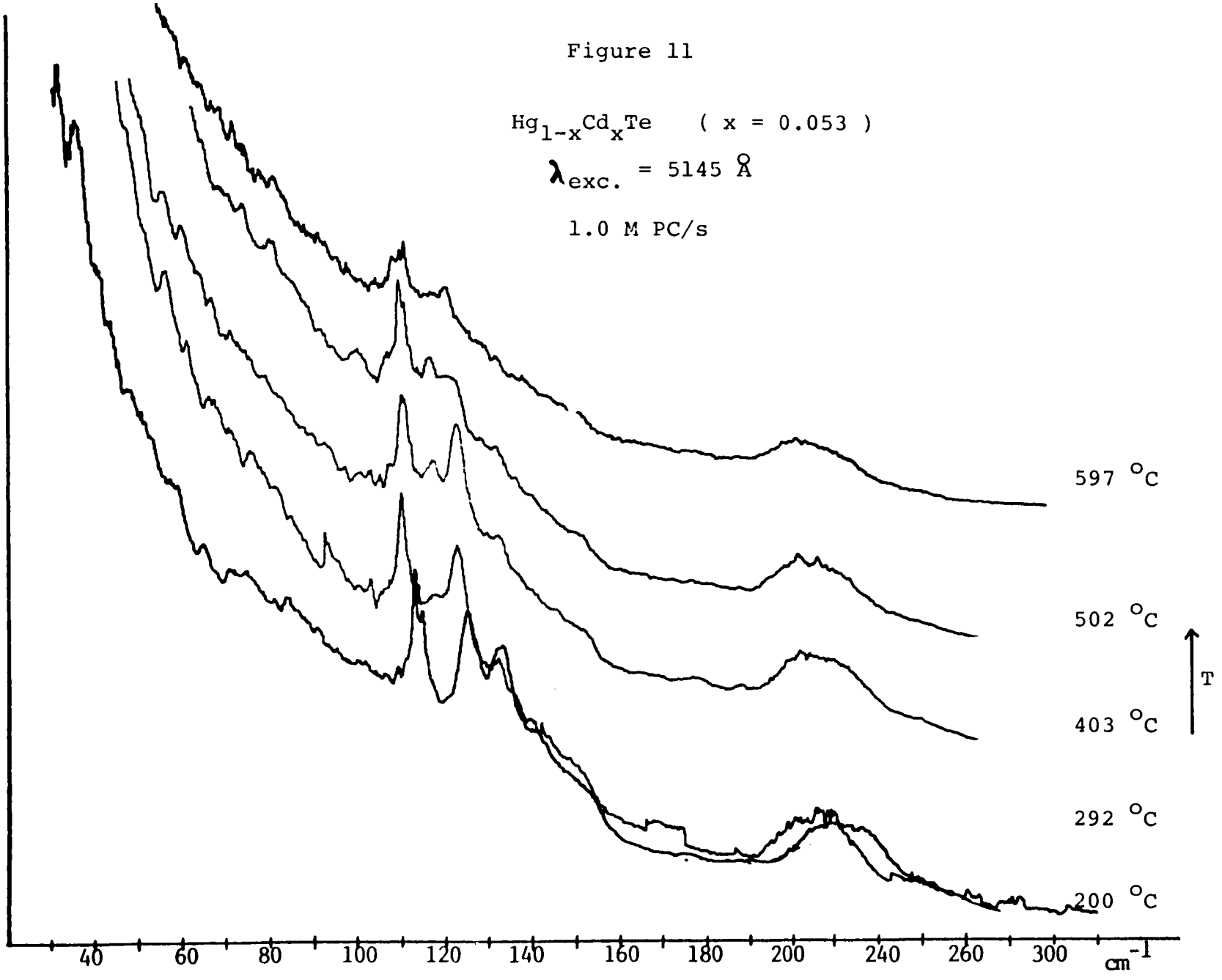

Figure 12

$Hg_{1-x}Cd_xTe$ (x = 0.053)

$\lambda_{exc.}$ = 5145 Å

1.0 M PC/s

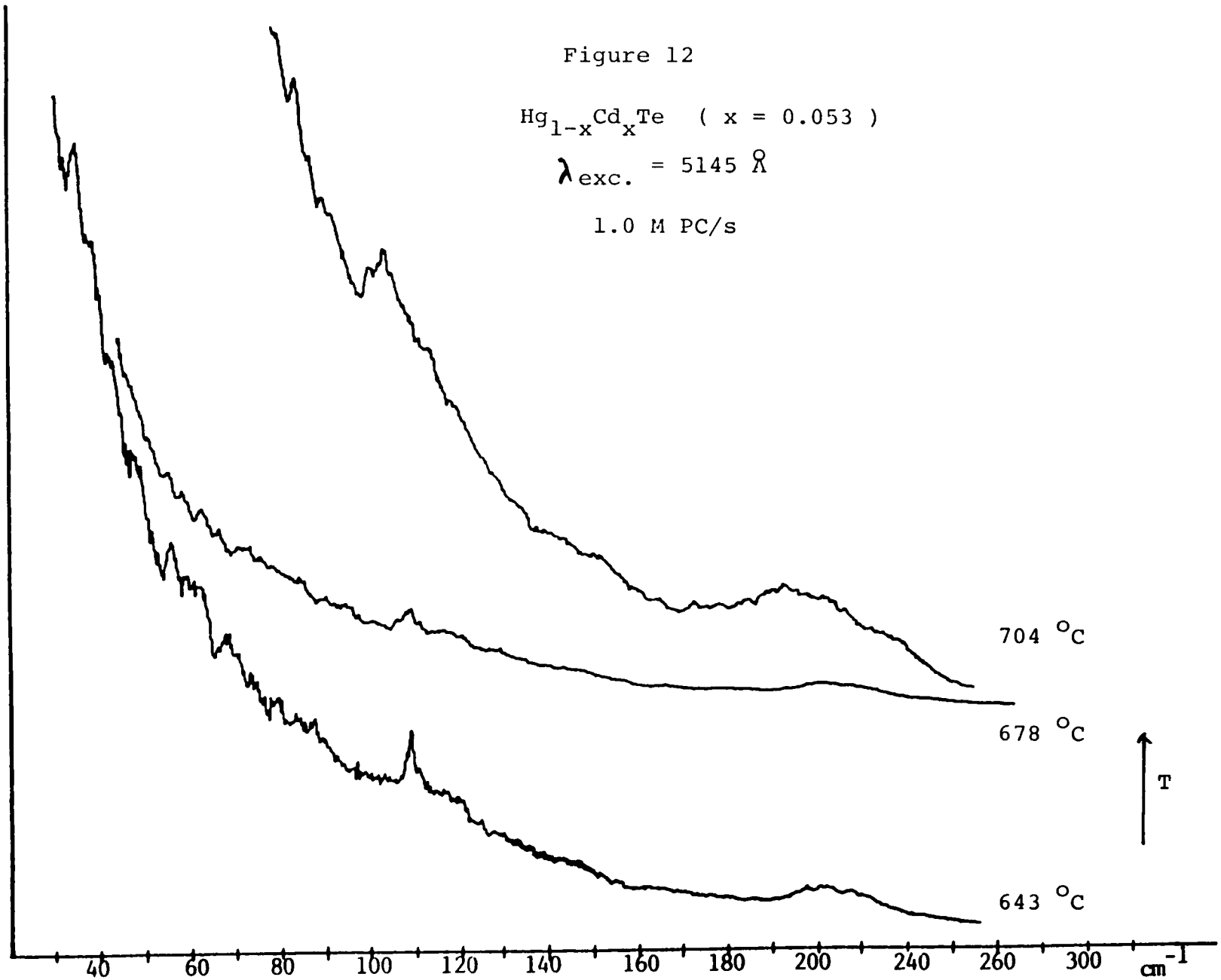

Figure 13

$Hg_{1-x}Cd_xTe$ (x = 0.053)

$\lambda_{exc.}$ = 5145 Å

1.0 M PC/s

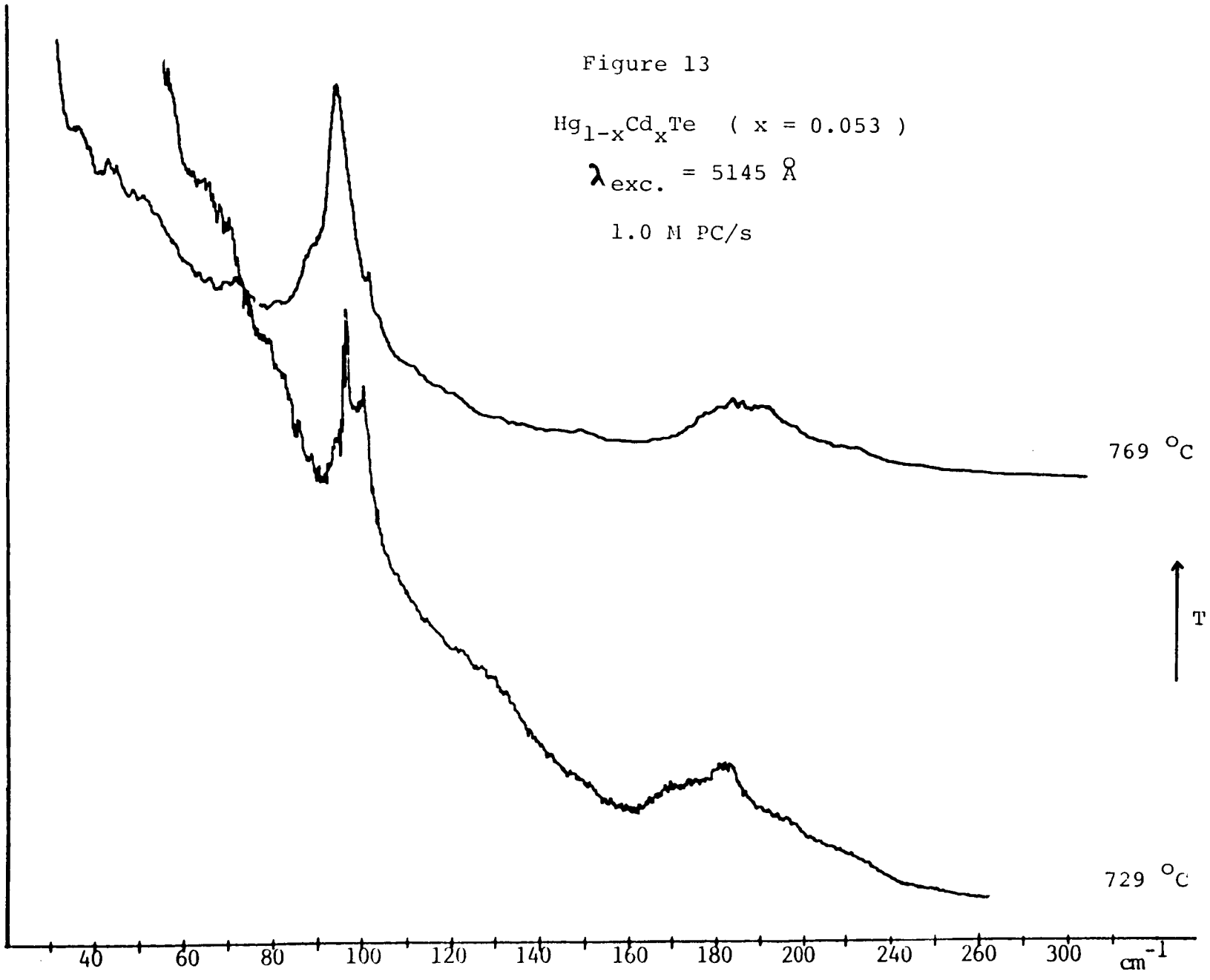

Figure 14

$Hg_{1-x}Cd_xTe$ (x = 0.053)

$\lambda_{exc.}$ = 5145 Å

1.0 M PC/s

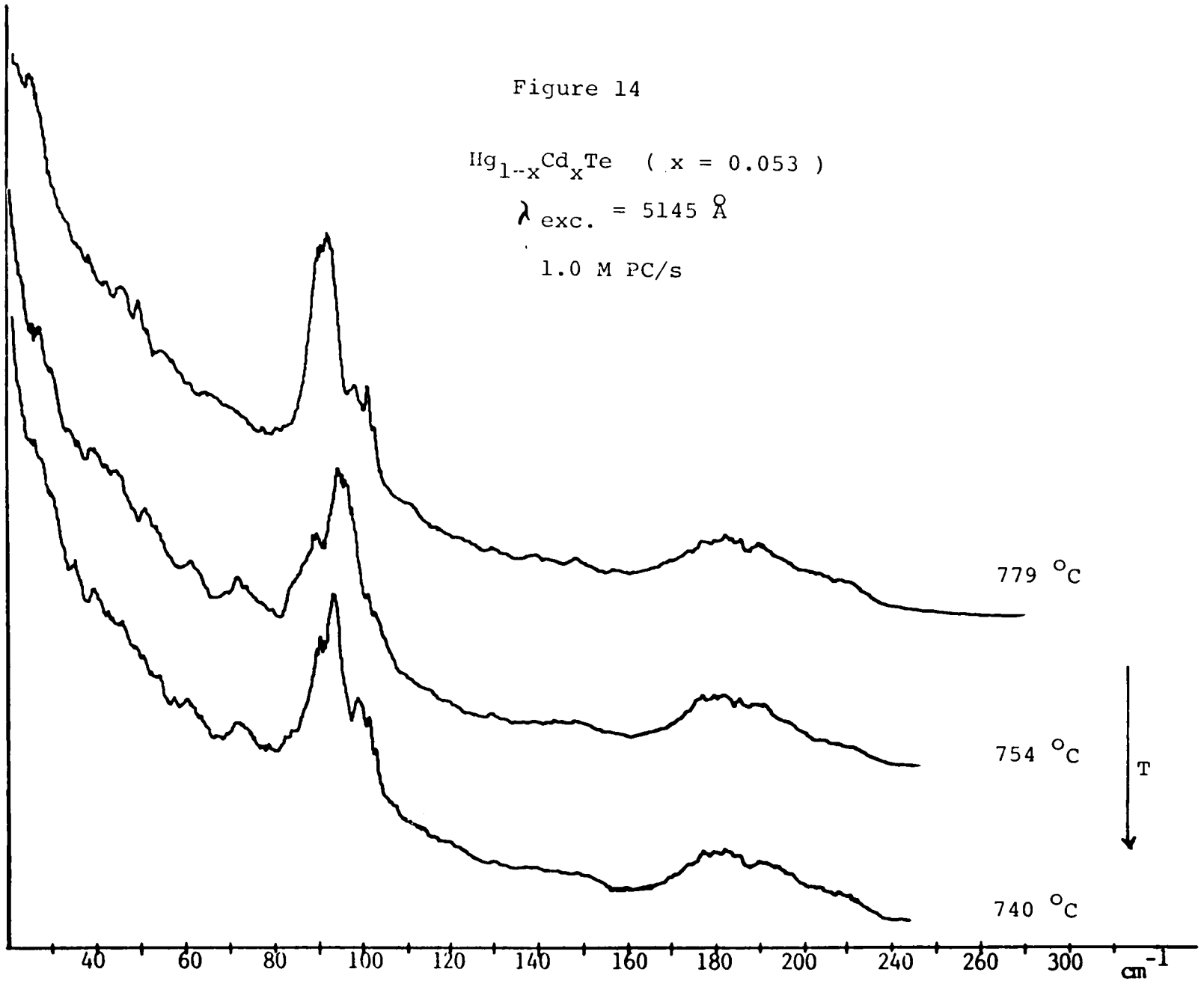

C. $Hg_{0.796}Cd_{0.204}Te$

The Raman spectra as a function of temperature for this 20% Cd composition sample are presented in Figures 15 through 18. Chronologically, this was the first sample on which the series of experiments were performed; it also produced the most dramatic signal enhancements with increased temperature. The spectra shown in Figure 15 were recorded with a spectral bandpass of 2.5 cm^{-1} and an incident laser power of 400 mW. The Raman signals were not easily detected as the temperature of the sample was increased, particularly for the series of spectra recorded between 106 ^{o}C and 500 ^{o}C. During this run we observed the first shifts in the scattered signal light relative to the entrance slit. Because these shifts caused significant decreases in the total collected signal, it was deemed necessary to maximize this amount (by increasing the slit withds) at the expense of a greater spectral bandpass. All subsequent spectra were then recorded under the same conditions. As seen in Figure 17, the intensity of the band at 128 cm^{-1} increases between 765 ^{o}C and 853 ^{o}C, decreases in intensity when the temperature is lowered to 750 ^{o}C, and does so by a factor of two when a temperature of 691 ^{o}C is attained.

D. $Hg_{0.70}Cd_{0.30}Te$

Only room temperature spectra were recorded for this alloy composition. The only difference between the room temperature spectra of the 20% sample and this 30% sample is that the latter exhibits weaker intensities for the same signals. Consequently, it was the last sample to be run for the series and not fully completed.

Figure 15

$Hg_{1-x}Cd_xTe$ (x = 0.204)

$\lambda_{exc.}$ = 5145 Å

20.0 K PC/s

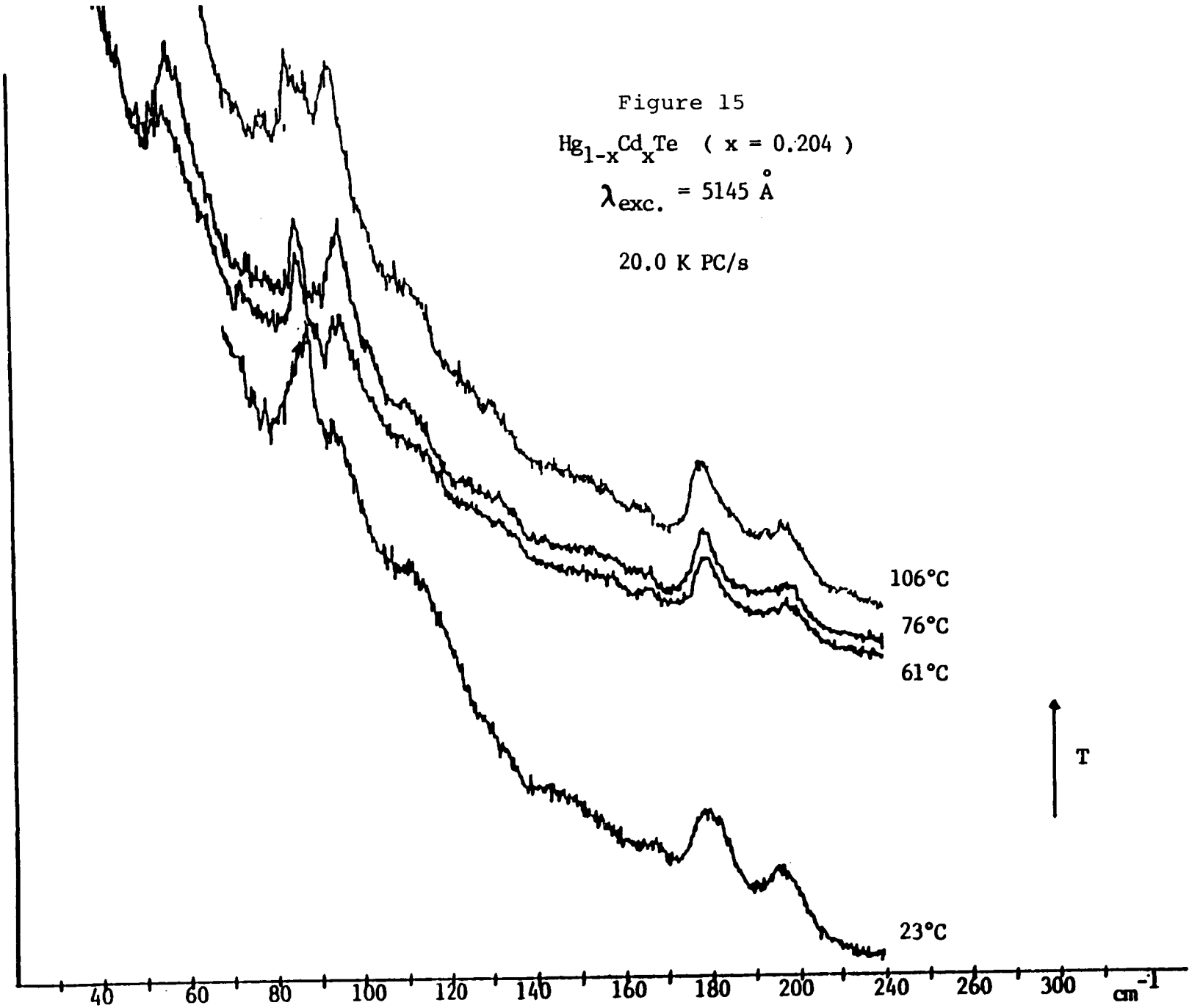

Figure 16

$Hg_{1-x}Cd_xTe$ (x = 0.204)

$\lambda_{exc.}$ = 5145 Å

1.0 M PC/s

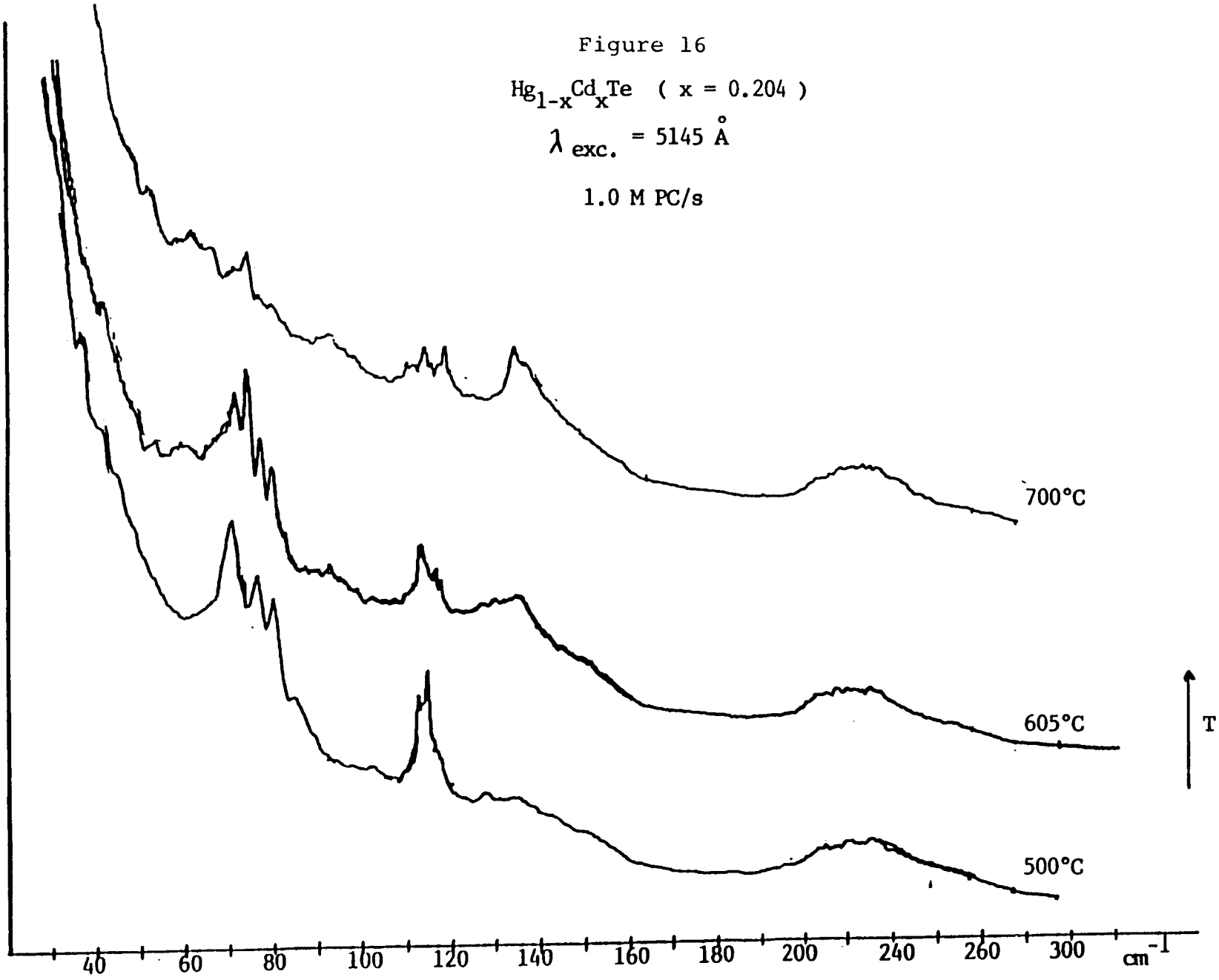

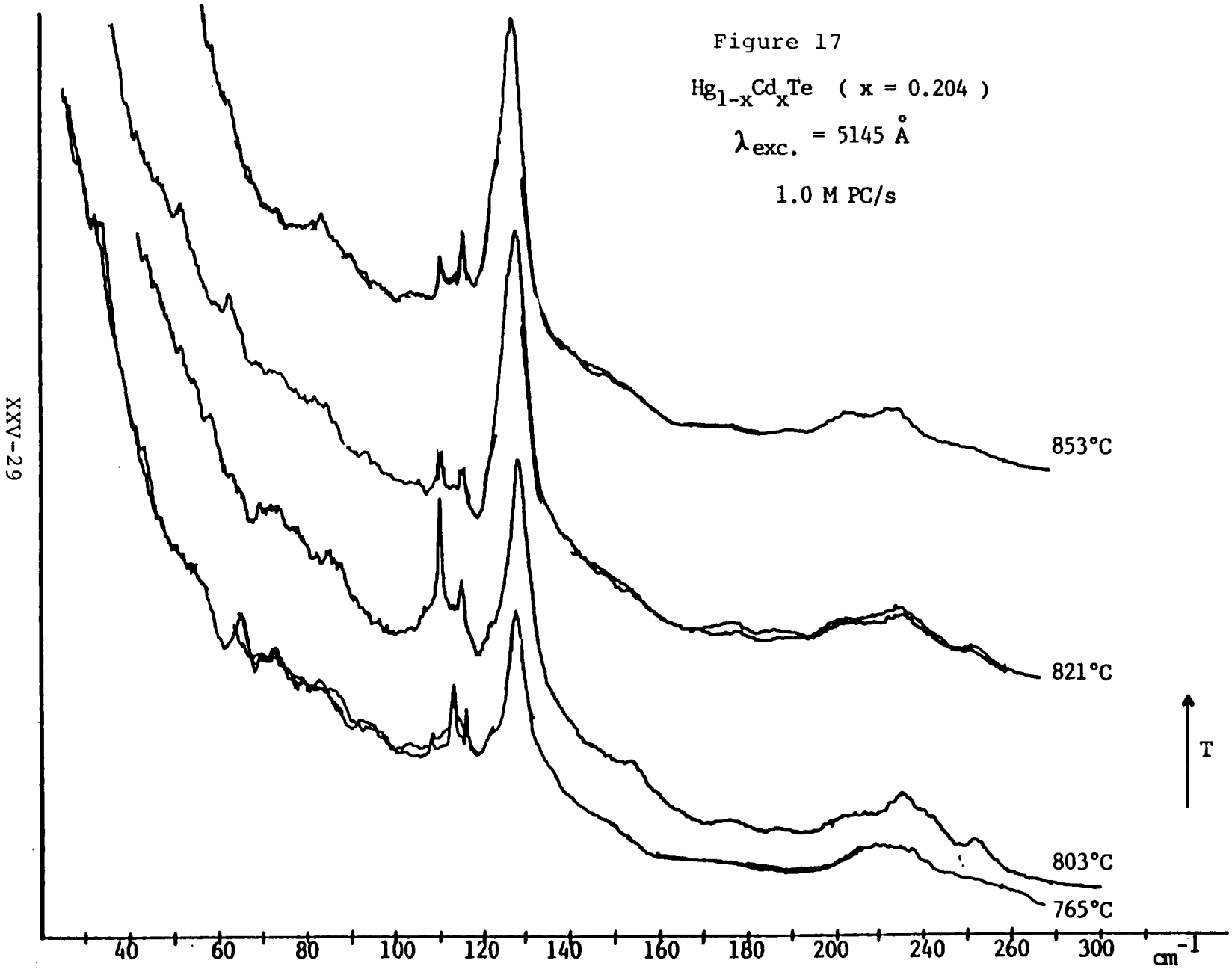
Figure 17
$Hg_{1-x}Cd_xTe$ (x = 0.204)
$\lambda_{exc.}$ = 5145 Å
1.0 M PC/s
XXV-29
853°C
821°C
803°C
765°C
T
40
60
80
100
120
140
160
180
200
240
260
300
cm-1

Figure 18

$Hg_{1-x}Cd_xTe$ (x = 0.204)

$\lambda_{exc.}$ = 5145 Å

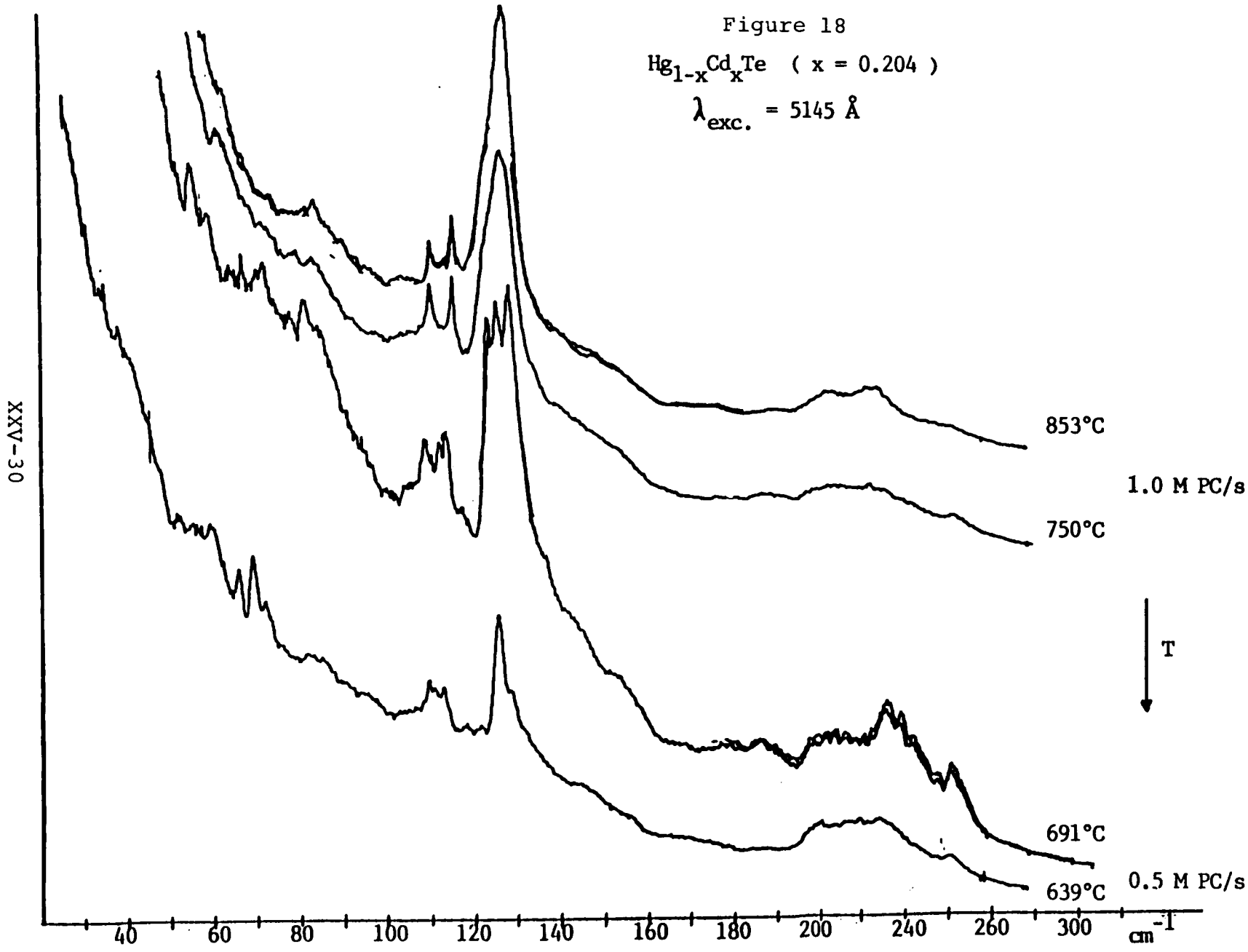

CONCLUSION

We have presented Raman scattering data for Hg-rich $Hg_{1-x}Cd_xTe$ melts. The spectra exhibit dramatic intensity enhancements for modes which can be associated with structural phase transitions for each sample composition studied. This argument is consistent with those previously suggested by others[6-11] to explain changes in thermal conductivities,[6-10] and in thermal diffusivity.[10,11] The measurements performed thus far do not indicate a soft-phonon mediated mechanism for this transition, although a 35 cm^{-1} shift to lower frequency was detected for the 5% Cd composition sample near its liquidus temperature.

These results are indeed very encouraging, but more needs to be done to complete the study. These measurements should be repeated for the same samples under similar conditions with shorter temperature intervals. This would aid in establishing the temperature width of the transition. In addition, the same experiments should also be performed for different excitation frequencies to confirm the phonon mode frequencies. This can be achieved by using the 4880 A line of the Ar^+ ion laser used for these experiments. If this option is used, every precaution must be taken to assure that a direct change of excitation frequency from the laser does not alter the optical path of the incident light. A better solution would be to use a completely different laser source, such as a He-Ne or Kr^+ laser, which can be positioned such that the optical paths are not disturbed other than by switching one mirror to reflect either one of the two incident beams.

These changes do not affect an important element in the detection and analysis of the data, and that is the strong background scattering that is observed for all of these materials. A computer data acquisition/control interface to the digital photon counter and program should help in the analysis of the data. The scattered background can then be digitally subtracted from the recorded spectrum leaving only the relevant part of the spectrum.

In conclusion, the preliminary results presented here are important for they represent the first observation of Raman scattering in Hg-Cd-Te melts. These efforts need to be enhanced with the above suggestions to confirm the observed phonon frequencies associated with the structural transitions, and to develop theoretical arguments to interpret the data within the framework of those previously presented for resonance Raman studies in these materials[27].

REFERENCES

1. R. Dornhaus and G. Nimtz, in "Springer Tracts in Modern Physics, Solid State Physics", vol. 78, ed. by G. Hohler, Springer-Verlag, Berlin, 1976, P. 1 and references therein.

2. R. K. Willardson and A. E. Beer, eds., "Semiconductors and Semimetals", vol. 18, Academic Press, New York, 1981.

3. R. Dornhaus and G. Nimtz, in "Narrow Gap Semiconductors", Springer Tracts in Modern Physics, vol. 98, ed. by G. Hohler and E. A. Niekish, Springer-Verlag, Berlin, 1983, p. 119 and references therein.

4. W. D. Lawson, et. al., J. Phys. Chem. Sol. **9** (1959) 325.

5. S. L. Lehoczky, F. R. Szofran, and B. G. Martin, "Advance Methods for Preparation and Characterization of Infrared Detector Materials, Part I", NASA CR-161598, 1980, and references therein.

6. S. L. Lehozcky and F. R. Szofran, "Advanced Methods for Preparation and Characterization of Infrared Detector Devices, Part II", NASA CR-161949, 1981, and references therein.

7. S. L. Lehoczky and F. R. Szofran, in "Materials Processing in the Reduced Gravity Environment of Space", ed. by G. E. Rindne, North-Holland Publishing, Amsterdam, 1982, p.409.

8. P. Capper, et. al., J. Cryst. Growth **63** (1983) 154.

9. L. R. Holland, "Space Processing of Electronic Materials", NASA CR-170653, 1982.

10. L. R. Holland and R. E. Taylor, J. Vac. Sci. Technol. **A1** (1983) 1615.

11. F. R. Szofran and S. L. Lehoczky, J. Cryst. Growth **70** (1984) 349.

12. D. L. Carter, M. A. Kinch, D. D. Buss, in "The Physics of Semimetals and Narrow-Gap Semiconductors", ed. by D. L. Carter and R. T. Bate, Pergamon Press, Oxford, 1971, p.273.

13. J. Baars and F. Sorger, Solid State Commun. **10** (1972) 875.

14. R. S. Kim and S. I. Narita, J. Phys. Soc. Japan **31** (1971) 613.

15. A. Polian, R. LeToullec and M. Balkanski, Phys. Rev. **B13** (1976) 3558.

16. M. Odet, et. al., Phys. Stat. Solidi **b92** (1979) 545.

17. S. P. Kozyrev, L. K. Vodopyanov and R. Triboulet, Solid State Commun. **45** (1983) 383.

18. S. P. Kozyrev, L. K. Vodopyanov and R. Triboulet, Sov. Phys. Solid State **25** (1983) 361.

19. S. C. Shen, J. H. Chu and H. J. Ye, in "Proceedings of the 17th International Conference on the Physics of Semiconductors", ed. by J. D. Chadi and W. A. Harrison, Springer-Verlag, New York, 1984, p. 1189.

20. D. N. Talwar and M. Vandevyver, J. Appl. Phys. **56** (1984) 1601.

21. L. K. Vodopyanov, et. al., in "Proceedings of the 17th International Conference on the Physics of Semiconductors", ed. by J. D. Chadi and W. A. Harrison, Springer-Verlag, New York, 1984, p. 947.

22. A. Mooradian and T. C. Harman, in" The Physics of Semimetals and Narrow-Gap Semiconductors", ed. by D. L. Carter and R. T. Bate, Pergamon Press, Oxford, 1971, p. 297.

23. P. M. Armitharaj, et. al., in "Proceedings of the 17th International Conference on the Physics of Semiconductors", ed. by J. D. Chadi and W. A. Harrison, Springer-Verlag, New York, 1984, p. 1397.

24. P. M. Amirtharaj, K.-K. Tiong, and F. H. Pollak, J. Vac Sci. Technol. **A1** (1983) 1744.

25. K.-K. Tiong, et. al., Solid State Commun. **50** (1984) 891.

26. P. M. Amirtharaj, et. al., J. Vac Sci. Technol. **A3** (1985) 226.

27. J. Menendez, M. Cardona, and L. K. Vodopyanov, Phys. Rev. **B31** (1985) 3705.

28. D. J. Olego, J. P. Faurie, and P. M. Raccah, Phys. Rev. Lett. **55** (1985) 328.

29. Y. A. Aleshchenko and L. K. Vodopyanov, Sov. Phys. Solid State **28** (1986) 1623.

30. G. Lucovsky, M. H. Brodsky and E. Burstein, Bull. Am. Phys. Soc. **15** (1970) 382.

31. C. V. Raman and T. M. K. Nedungadi, Nature **145** (1940) 147.

32. J. F. Scott, Rev. Mod. Phys. **46** (1974) 83.

33. D. M. Hanson, J. Chem. Phys. **63** (1975) 5046.

34. W. Hayes and R. Loudon, "Scattering of Light by Crystals", Wiley-Interscience, New York, 1978.

35. A. Anderson, ed., "The Raman Effect", Marcel-Dekker, New York, vol. 1, 1971, and vol. 2, 1973.

36. Advances in Raman Spectroscopy **1** (1971) and subsequent volumes of this periodical.

37. M. Balkanski, in "Narrow-Gap Semiconductors: Physics and Applications", ed. by W. Zawadzki, Lecture Notes in Physics, vol. 133, Springer-Verlag, Berlin, 1980, p. 67.

38. M. Cardona, in "Light Scattering in Solids II", ed. by M. Cardona and G. Guntherodt, Springer-Verlag, Heidelberg, 1982, p. 19.

39. A. Compaan and H. J. Trodahl, Phys. Rev. **B29** (1984) 793.

40. J. Menendez and M. Cardona, Phys. Rev. **B31** (1985) 3696.

41. W. Kauschke and M. Cardona, Phys. Rev. **B35** (1987) 9619.

42. C. V. Raman and K. S. Krishnan, Nature **121** (1928) 501.

43. J. Behringer, in "Molecular Spectroscopy", ed. by R. F. Barrow, D. A. Long and D. J. Millen, Specialist Periodical Reports, vol. 2,, The Chemical Society, London, 1974, p. 100.

44. L. R. Holland, R. P. Harris and R. Smith, Rev. Sci. Instrum. **54** (1983) 993.

45. J. M. Zwiener, personal communication.

46. G. L. Workman, "Vapor Transport Mechanisms", Final Report, NASA Contract NAS8-31731, 1978.

47. R. C. Hawes, et. al., Anal. Chem. **38** (1966) 1842.

48. J. R. Scherer, G. F. Briley and S. Kint, Anal. Chem. **43** (1971) 1917.

49. D. F. Shriver and J. B. R. Dunn, Appl. Spec. **28** (1974) 319.